Inorganic Chemistry

pubs.acs.org/IC

Communication

Effect of Equatorial Ligand Substitution on the Reactivity with Proteins of Paddlewheel Diruthenium Complexes: Structural Studies

Aarón Terán, Giarita Ferraro, Ana E. Sánchez-Peláez, Santiago Herrero,* and Antonello Merlino*

Cite This: *Inorg. Chem.* 2023, 62, 670−674

Read Online

ACCESS | Metrics & More | Article Recommendations | Supporting Information

ABSTRACT: The paddlewheel $[Ru_2Cl(O_2CCH_3)_4]$ complex was previously reported to react with the model protein hen egg white lysozyme (HEWL), forming adducts with two diruthenium moieties bound to Asp101 and Asp119 side chains upon the release of one acetate. To study the effect of the equatorial ligands on the reactivity with proteins of diruthenium compounds, X-ray structures of the adducts formed when HEWL reacts with $[Ru_2Cl(D\text{-}p\text{-}FPhF)(O_2CCH_3)_3]$ [D-*p*-FPhF = *N*,*N*′-bis(4-fluorophenyl)formamidinate] under different conditions were solved. $[Ru_2Cl(D\text{-}p\text{-}FPhF)(O_2CCH_3)_3]$ is bonded through their equatorial positions to the Asp side chains. Protein binding occurs cis or trans to D-*p*-FPhF. Lys or Arg side chains or even main-chain carbonyl groups can coordinate to the diruthenium core at the axial site. Data help to understand the reactivity of paddlewheel diruthenium complexes with proteins, providing useful information for the design of new artificial diruthenium-containing metalloenzymes with potential applications in the fields of catalysis, biomedicine, and biotechnology.

Most of the diruthenium complexes with the general formula $[Ru_2X(L{-}L)_4]$ contain a strong metal−metal interaction (bond order of 2.5), four bridging equatorial ligands (L−L) arranged in a lantern-like fashion around the dimetallic center, and donor ligands (X) at the axial positions.[1−3] These molecules have attracted considerable interest for their application in catalysis[4−10] or biomedicine[11] and for their peculiar magnetic and redox properties.[12−14]

The prototype of the diruthenium compounds family, $[Ru_2Cl(O_2CCH_3)_4]$, has interesting pharmaceutical properties and has been used as a precursor to prepare promising anticancer compounds.[11,15−17] For example, diruthenium compounds containing nonsteroidal antiinflammatory drugs[18−20] or γ-linolenic acid[21,22] as ligands have been found to be active against glioma tumor models *in vitro* and *in vivo* and, in particular, against human glioblastoma cell lines, while the $[Ru_2Cl(EB776)_4]$ complex [where EB776 is the deprotonated form of (2-phenylindol-3-yl)glyoxyl-L-phenylalanine-L-leucine] was found to be active against a glioblastoma cell line.[23] The diruthenium ibuprofenate complex also shows antiinflammatory properties with reduced gastric ulceration *in vivo* compared to the copper ibuprofenate complex.[24]

In earlier work, the interaction of $[Ru_2Cl(O_2CCH_3)_4]$ with the model protein hen egg white lysozyme (HEWL) was studied to give the first key insights into the biological targets and mode of action of the diruthenium metallodrugs: the diruthenium center binds the protein, retaining the Ru−Ru bond and replacing one acetate ligand by an Asp side chain; a second acetate is then replaced by two water (H_2O) molecules.[25]

Recently, it has been suggested that the use of bulky equatorial substituents on the diruthenium core may constitute an approach to increase the selectivity of diruthenium complexes toward anticancer targets.[26,27] Many diruthenium complexes of the type $[Ru_2Cl(L{-}L)_4]$ (L−L = *O*,*N* donors,[28,29] *N*,*N*′-donors[30,31] or other *O*,*O*′-donors[3,32]) have been synthesized. However, intermediate substitution species $[Ru_2Cl(L{-}L)_x(O_2CCH_3)_{4-x}]$ (x = 1−3) are quite scarce.[14,33−35] These molecules show variations in the stability, solubility, redox potential, and paramagnetic behavior compared to $[Ru_2Cl(O_2CCH_3)_4]$ and to their fully substituted species.

Here, we investigate interaction of the monosubstituted diruthenium compound $[Ru_2Cl(D\text{-}p\text{-}FPhF)(O_2CCH_3)_3]$, where D-*p*-FPhF = *N*,*N*′-bis(4-fluorophenyl)formamidinate (Figure 1), with HEWL under four different experimental conditions. $[Ru_2Cl(L{-}L)(O_2CCH_3)_3]$ compounds are soluble in H_2O and are expected to be more stable than $[Ru_2Cl(O_2CCH_3)_4]$ according to the previous results.[34]

X-ray structures of adducts formed upon reaction of the protein with $[Ru_2Cl(D\text{-}p\text{-}FPhF)(O_2CCH_3)_3]$ are reported. The results are compared with those obtained when proteins react with $[Ru_2Cl(O_2CCH_3)_4]$[25] and various dirhodium compounds.[36−40] The stability of $[Ru_2Cl(D\text{-}p\text{-}FPhF)(O_2CCH_3)_3]$ was first studied in solution by UV−vis absorption spectroscopy (Figure 2). The spectrum in dichloromethane showed only one transition band around 480 nm.[34] However, in H_2O, the electronic spectrum shows bands in the UV (243 and 338 nm) and visible (∼420 and 520 nm) regions. A recent study by Kadish and co-workers[41] with similar compounds showed the sensitivity of the axial positions to

Received: November 21, 2022
Published: January 4, 2023

https://doi.org/10.1021/acs.inorgchem.2c04103
Inorg. Chem. 2023, 62, 670−674

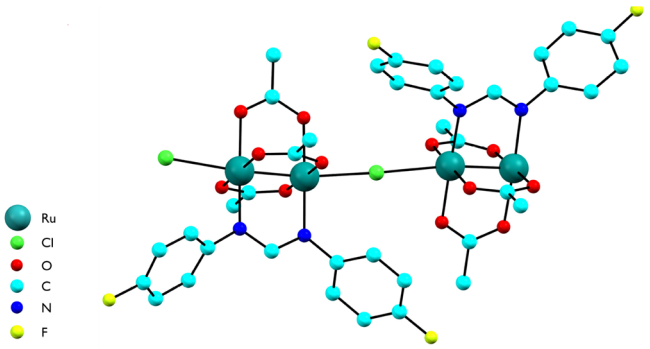

Figure 1. Asymmetric unit of $[Ru_2Cl(D\text{-}p\text{-}FPhF)(O_2CCH_3)_3]_n \cdot 2nCH_2Cl_2$. Solvent molecules and H atoms have been omitted for clarity.

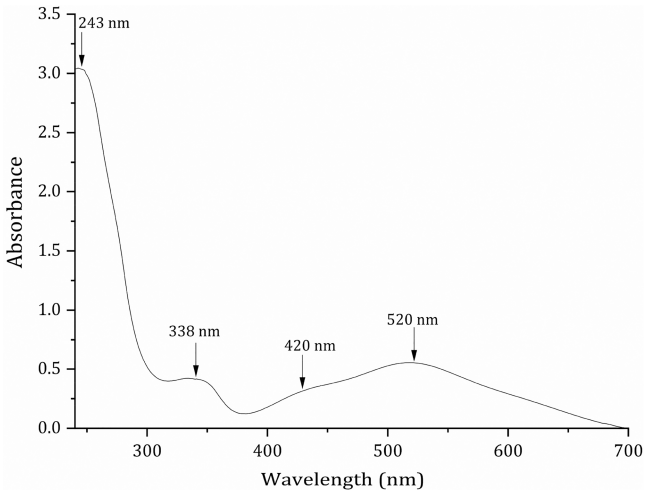

Figure 2. Time course UV−vis spectra of 50 μM $[Ru_2Cl(D\text{-}p\text{-}FPhF)(O_2CCH_3)_3]$ in Milli-Q water. No appreciable spectral changes were observed within 24 h.

donor ligands [H_2O or dimethyl sulfoxide (DMSO)] and suggested coordination to the axial positions.

The higher-energy UV band is usually assigned to an axial ligand-to-metal charge transfer.[42] The peak at 338 nm can be assigned to ligand-to-metal transitions [π(N) → $\sigma^*/\pi^*/\delta^*(Ru_2)$], while the peaks in the visible region can be assigned to an allowed ligand-to-metal charge transfer [π(N), π(axial) → $\pi^*(Ru_2)$].[41] These signals do not experience any change after 24 h.

UV−vis spectra of $[Ru_2Cl(D\text{-}p\text{-}FPhF)(O_2CCH_3)_3]$ were also collected in the conditions that are used to grow HEWL crystals in the absence (Figures S1A−D) and presence of HEWL (protein to diruthenium compound molar ratio of 1:3; Figures S2A−D). In almost all of the conditions used for the crystallization experiments, ignorable variations in the spectral profiles of the compound are observed, while minimal variations are found in the presence of HEWL (Figures S1A−D and S2A−D). These findings suggest that the diruthenium compound is more stable than $[Ru_2Cl(O_2CCH_3)_4]$ in different aqueous solutions[25] and could bind the protein.

Circular dichroism spectra of the protein in the absence and presence of diruthenium are superimposable, with negligible variations of the molar ellipticity (Figure S3). These data suggest that HEWL retains its secondary structure and is presumably well-folded in the presence of $[Ru_2Cl(D\text{-}p\text{-}FPhF)(O_2CCH_3)_3]$.

Fluorescence data confirm that the diruthenium compound binds the protein; indeed, a quenching of the intrinsic fluorescence of HEWL is observed when the metal compound concentration is increased (Figure S4A−F). The quenching is not accompanied by a change of the maximum emission wavelength, thus suggesting that metal compound binding occurs without the overall protein structure being altered.

Crystals of the adducts formed upon incubation of the protein with the metal compound were obtained by a soaking procedure under four different experimental conditions (see the Supporting Information for further details). The resolution of the structures ranges from 1.07 to 1.81 Å. Data collections and refinement statistics are reported in Table S1. The structures of the protein in the four adducts are very similar to

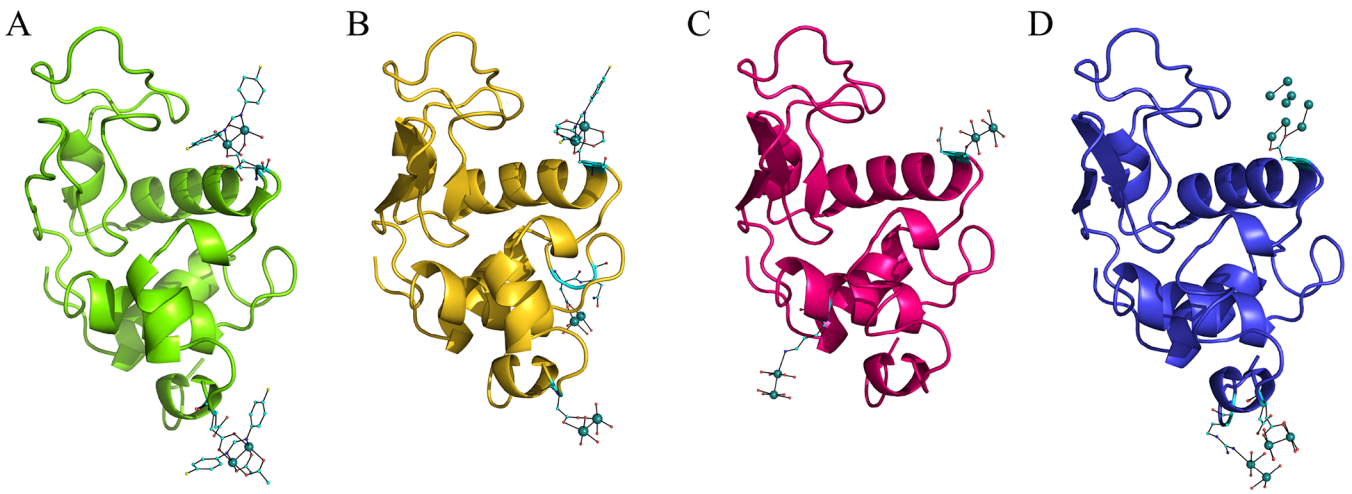

Figure 3. Overall structures of the adducts formed in the reaction of $[Ru_2Cl(D\text{-}p\text{-}FPhF)(O_2CCH_3)_3]$ with HEWL under different experimental conditions: (A) structure **1** (20% ethylene glycol, 0.1 M sodium acetate buffer at pH 4.0, and 0.6 M sodium nitrate); (B) structure **2** (2.0 M sodium formate and 0.1 M HEPES buffer at pH 7.5); (C) structure **3** (0.8 M succinic acid at pH 7.0); (D) structure **4** (1.1 M sodium chloride and 0.1 M sodium acetate buffer at pH 4.0). Coordinates and structure factors are deposited in the PDB with codes 8BPH (structure **1**), 8BPU (structure **2**), 8BPJ (structure **3**), and 8BQM (structure **4**). Ru atoms are in green.

https://doi.org/10.1021/acs.inorgchem.2c04103
Inorg. Chem. 2023, 62, 670−674

each other and are not significantly affected by interaction with the metal compound (Figure 3). The root-mean-square deviation of Cα atoms from the structure of the metal-free protein (PDB code 193L)[43] is within the range 0.17−0.21 Å.

In structure **1** (Figure 3A), diruthenium centers are found to be close to the side chains of Asp101 or Asp119 (Figures 4A,B). The diruthenium-containing fragment bound close to Asp119 is well-defined (Figure 4B), while the D-*p*-FPhF ligand of the diruthenium bound to Asp101 is less ordered (Figure 4A). The two diruthenium-containing fragments are alternative to each other with 0.50 and 0.40 occupancies, respectively. The Asp119 side chain changes its conformation to coordinate the diruthenium center at the equatorial site (Figure S5), while Asp101 is already in the right position in the metal-free protein to link the dimetallic center. Close to the Asp119 side chain, the diruthenium unit binds two acetate ligands along with one L−L bridging ligand and the carboxylate group of Asp at the equatorial position. Close to the Asp101 side chain, acetate ligands could be replaced by H_2O molecules. Because of the crystallization conditions (low pH and high concentration of sodium nitrate), we cannot exclude that, in structure **1**, acetate ligands were replaced by nitrate ions. The axial positions of the diruthenium center bound to Asp119 are occupied by H_2O molecules, while at the Asp101 binding site, axial ligands were not added to the model because of low electron density.

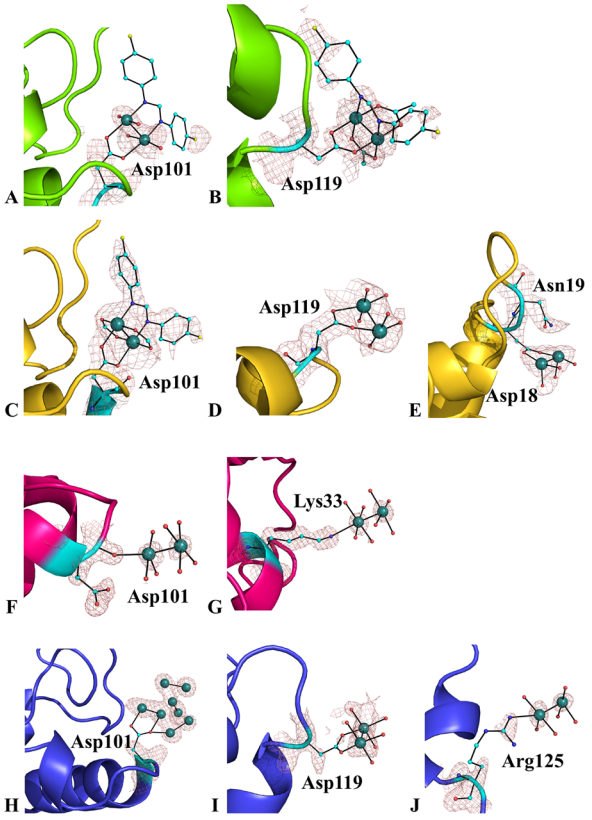

Figure 4. Diruthenium binding sites in the adducts formed upon the reaction of HEWL with $[Ru_2Cl(D\text{-}p\text{-}FPhF)(O_2CCH_3)_3]$ in structures **1** (panels A and B), **2** (panels C−E), **3** (panels F and G), and **4** (panels H−J). The electron density maps are very well-defined and unambiguously indicate that the compound retains the diruthenium center and L−L ligands upon protein binding. Axial H_2O molecules are omitted for the sake of clarity. $2F_o - F_c$ electron density maps are contoured at 1.0 σ (salmon).

Notably, close to Asp119, the diruthenium-containing fragment binds the Asp side chain cis to the D-*p*-FPhF ligand, while close to Asp101, the side chain is trans to the L−L ligand. As was already observed, bisubstituted species usually have cis configuration. The trans disposition has only been obtained with bulky equatorial ligands.[14]

In structure **2** (Figure 3B), similar results were obtained (Figure 4C−E): the diruthenium center binds Asp101, with the side chain trans to the L−L ligand (occupancy = 0.70; Figure 4C) and to Asp119 (occupancy = 0.55; Figure 4D). Interestingly, in this structure, the diruthenium bound to Asp101 with the side chain trans to the D-*p*-FPhF ligand (Figure 4C) is better defined than that bound to Asp119 (Figure 4D). In the former diruthenium binding site, inspection of the electron density maps suggests that two formate ions have replaced acetate ligands (Figure 4C). Axially coordinated H_2O molecules can also be confidently modeled. In the latter, the electron density is disordered and diruthenium ligands have been interpreted as H_2O molecules (Figure 4D). An additional diruthenium binding site with low occupancy (0.20) is found to be close to the side chain of Asp18 (Figure 4E). Here, only two Ru atoms and a few H_2O molecules as ligands have been modeled. The Ru atoms are at ∼3 Å from the atoms of the Asn19 side chain.

Additional binding sites for the diruthenium core were found also in structure **3** (Figure 3C). In this structure, a diruthenium center is axially coordinated to the carbonyl of Asp101 (Figure 4F) and to the Lys33 side chain (Figure 4G). Unfortunately, in both of these additional diruthenium binding sites, metal ligands cannot be confidently modeled because of the low occupancy of the metal (0.25 and 0.20, respectively) and conformational disorder. The carbonyl group probably competes with H_2O molecules in solution. Nevertheless, the axial coordination of dimetallic compounds to both a residue side chain and a carbonyl oxygen in the solid state was already observed in the adducts formed upon the reaction of dirhodium compounds with proteins.[36−40,44]

In structure **4** (Figure 3D), binding of the dimetallic center occurs at the level of the side chains of Asp101 (Figure 4H), Asp119 (Figure 4I), and Arg125 (Figure 4J). However, in this structure, especially close to the side chain of Asp101 (Figure 4H), interpretation of the map is complicated by conformational disorder, by the presence of multiple conformations of the diruthenium center, and by the presence of a high concentration of chloride ions, which could replace the diruthenium ligands.[45] Interestingly, the diruthenium center close to the side chain of Arg125 is axially coordinated (Figure 4J).

Overall, these data indicate that Ru−Ru bonds remain stable upon reaction with HEWL regardless of the experimental conditions used. Interestingly, the structures of the adducts of HEWL with dirhodium tetraacetate and derivatives under the same conditions show breakage of the Rh−Rh bond.[36,38,39]

In conclusion, here we have studied the reactivity of $[Ru_2Cl(D\text{-}p\text{-}FPhF)(O_2CCH_3)_3]$ with HEWL under different experimental conditions. Our data unambiguously demonstrate that the compound binds the protein, forming adducts with dimetallic moieties bound to the Asp side chains upon the release of an acetate ligand. In the adduct, excluding the acetate replaced by the Asp side chain, the other ligands can be retained and the D-*p*-FPhF ligand can be cis or trans to the Asp side chain probably due to steric hindrance. These data confirm that diruthenium compounds react with proteins,

https://doi.org/10.1021/acs.inorgchem.2c04103
Inorg. Chem. 2023, 62, 670−674

forming adducts with Asp side chains at equatorial sites[24] and keeping their paddlewheel structure. The results also indicate that monosubstituted diruthenium compounds present a different reactivity with proteins compared to diruthenium tetraacetate[25] and to paddlewheel dirhodium compounds.[36−40,44]

Our data also suggest the possibility of an axial bond of the diruthenium core to the side chains of Lys or Arg and to backbone carbonyl groups. It is possible that the binding of the Asp residues at the equatorial position is a late event in the reaction of paddlewheel complexes with proteins and that the coordination of protein nucleophile sites at the axial position of the bimetallic scaffolds can be an early event in the dimetallic compound/protein recognition process. The binding to the axial site not only anticipates the later acetate detachment but also could exert a structural destabilization that facilitates its eventual occurrence, as indicated by computational studies.[26] The combination of axial and equatorial coordinative binding has been postulated as a way to establish specific interactions between $[Ru_2Cl_2(formamidinate)_3(DMSO)]$ and ribonucleic acid.[46]

■ ASSOCIATED CONTENT

Supporting Information

The Supporting Information is available free of charge at https://pubs.acs.org/doi/10.1021/acs.inorgchem.2c04103.

Materials, solution studies, crystallization and X-ray structure solution and refinement, Figures S1−S5, and Table S1 (PDF)

■ AUTHOR INFORMATION

Corresponding Authors

Antonello Merlino − *Department of Chemical Sciences, University of Naples Federico II, Naples 80126, Italy;* orcid.org/0000-0002-1045-7720; Email: antonello.merlino@unina.it

Santiago Herrero − *Departamento de Química Inorgánica, Facultad de Ciencias Químicas, Universidad Complutense de Madrid, Madrid E-28040, Spain;* orcid.org/0000-0002-9901-1142; Email: sherrero@ucm.es

Authors

Aarón Terán − *Departamento de Química Inorgánica, Facultad de Ciencias Químicas, Universidad Complutense de Madrid, Madrid E-28040, Spain*

Giarita Ferraro − *Department of Chemical Sciences, University of Naples Federico II, Naples 80126, Italy*

Ana E. Sánchez-Peláez − *Departamento de Química Inorgánica, Facultad de Ciencias Químicas, Universidad Complutense de Madrid, Madrid E-28040, Spain*

Complete contact information is available at: https://pubs.acs.org/10.1021/acs.inorgchem.2c04103

Notes

The authors declare no competing financial interest.

■ ACKNOWLEDGMENTS

The authors thank the Elettra staff for technical assistance. Comunidad de Madrid is gratefully acknowledged for financial support (Project S2017/BMD-3770-CM). A.T. acknowledges the Universidad Complutense for a Predoctoral Grant (CT63/19-CT64/19) and Research Stay Grant (EB25/22) and the Spanish Ministry of Science and Innovation for a Postgraduate Fellowship at Residencia de Estudiantes (2021−2022).

■ REFERENCES

(1) Cotton, F. A.; Murillo, C. A.; Walton, R. A. *Multiple Bonds between Metal Atoms*, 3rd ed.; Springer: New York, 2005.

(2) Bennett, M. J.; Caulton, K. G.; Cotton, F. A. Structure of tetra-n-butyratodiruthenium chloride, a compound with a strong metal-metal bond. *Inorg. Chem.* **1969**, *8*, 1−6.

(3) Aquino, M. A. S. Recent developments in the synthesis and properties of diruthenium tetracarboxylates. *Coord. Chem. Rev.* **2004**, *248*, 1025−1045.

(4) Miyazawa, T.; Suzuki, T.; Kumagai, Y.; Takizawa, K.; Kikuchi, T.; Kato, S.; Onoda, A.; Hayashi, T.; Kamei, Y.; Kamiyama, F.; Anada, M.; Kojima, M.; Yoshino, T.; Matsunaga, S. Chiral paddle-wheel diruthenium complexes for asymmetric catalysis. *Nat. Catal.* **2020**, *3*, 851−858.

(5) Barker, J. E.; Ren, T. Diruthenium(II,III) Bis(tetramethyl-1,3-benzenedipropionate) as a novel catalyst for tert-butyl hydroperoxide oxygenation. *Inorg. Chem.* **2008**, *47*, 2264−2266.

(6) Kato, C. N.; Ono, M.; Hino, T.; Ohmura, T.; Mori, W. Room temperature oxidation of alcohols with 1 atm dioxygen and air catalyzed by a novel three-dimensional microporous ruthenium(II, III) 4,4′,4″,4‴-(21H,23H-porphine-5,10,15,20-tetrayl)-tetrakisbenzoate tetrafluoroborate. *Catal. Commun.* **2006**, *7*, 673−677.

(7) Harvey, M. E.; Musaev, D. G.; Du Bois, J. A diruthenium catalyst for selective, intramolecular allylic C-H amination: reaction development and mechanistic insight gained through experiment and theory. *J. Am. Chem. Soc.* **2011**, *133*, 17207−17216.

(8) Nakae, T.; Yasunaga, T.; Kamiya, M.; Fukumoto, Y.; Chatani, N. Skeletal reorganization of enynes catalyzed by a Ru(II)-Ru(III) mixed-valence complex under an atmosphere of O_2 or CO. *Chem. Lett.* **2013**, *42*, 1565−1567.

(9) Berry, F. Metal-metal multiple bonded intermediates in catalysis. *J. Chem. Sci.* **2015**, *127*, 209−214.

(10) Lupi, F.; Marzo, T.; D'Adamio, G.; Cretella, S.; Cardona, F.; Messori, L.; Goti, A. Diruthenium diacetate catalysed aerobic oxidation of hydroxylamines and improved chemoselectivity by immobilisation to lysozyme. *ChemCatalChem.* **2017**, *9*, 4225−4230.

(11) de Oliveira Silva, D. Perspectives for novel mixed diruthenium-organic drugs as metallopharmaceuticals in cancer therapy. *Anti-Cancer Agents Med. Chem.* **2010**, *10*, 312−32.

(12) Barral, M. C.; Herrero, S.; Jiménez-Aparicio, R.; Torres, M. R.; Urbanos, F. A. A Spin-Admixed Ruthenium Complex. *Angew. Chem., Int. Ed.* **2005**, *44*, 305−307.

(13) Cotton, F. A.; Herrero, S.; Jiménez-Aparicio, R.; Murillo, C. A.; Urbanos, F. A.; Villagrán, D.; Wang, X. How Small Variations in Crystal Interactions Affect Macroscopic Properties. *J. Am. Chem. Soc.* **2007**, *129*, 12666−12667.

(14) Angaridis, P.; Cotton, F. A.; Murillo, C. A.; Villagrán, D.; Wang, X. Paramagnetic precursors for supramolecular assemblies: selective syntheses, crystal structures, and electrochemical and magnetic properties of $Ru_2(O_2CMe)_{4-n}(formamidinate)_nCl$ complexes, n = 1−4. *Inorg. Chem.* **2004**, *43*, 8290−8300.

(15) van Rensburg, E. J.; Kreft, E.; Swarts, J. C.; Dalrymple, S. R.; MacDonald, D. M.; Cooke, M. W.; Aquino, M. A. S. Cytotoxicity of a series of water-soluble mixed valent diruthenium tetracarboxylates. *Anticancer Res.* **2002**, *22*, 889−892.

(16) Keppler, B. K.; Henn, M.; Juhl, U. M.; Berger, M. R.; Niebl, R.; Wagner, F. E. New ruthenium complexes for the treatment of cancer. *Prog. Clin. Biochem. Med.* **1989**, *10*, 41−69.

(17) Alves, S. R.; Santos, R. L. S. R.; Fornaciari, B.; Colquhoun, A.; de Oliveira Silva, D. A novel μ-oxo-diruthenium(III, III)-ibuprofen-(4-aminopyridine) chloride derived from the diruthenium(II,III)-ibuprofen paddlewheel metallodrug shows anticancer properties. *J. Inorg. Biochem.* **2021**, *225*, 111596.

(18) Ribeiro, G.; Benadiba, M.; Colquhoun, A.; de Oliveira Silva, D. Diruthenium(II,III) complexes of ibuprofen, aspirin, naproxen and indomethacin non-steroidal anti-inflammatory drugs: Synthesis,

characterization and their effects on tumor-cell proliferation. *Polyhedron* **2008**, *27*, 1131−1137.
(19) Benadiba, M.; dos Santos, R. R. P.; de Oliveira Silva, D.; Colquhoun, A. Inhibition of C6 rat glioma proliferation by $[Ru_2Cl(Ibp)_4]$ depends on changes in p21, p27, Bax/Bcl2 ratio and mitochondrial membrane potential. *J. Inorg. Biochem.* **2010**, *104*, 928−935.
(20) Hanif-Ur-Rehman; Freitas, T. E.; Gomes, R. N.; Colquhoun, A.; de Oliveira Silva, D. Axially-modified paddlewheel diruthenium-(II,III)-ibuprofenato metallodrugs and the influence of the structural modification on U87MG and A172 human glioma cell proliferation, apoptosis, mitosis and migration. *J. Inorg. Biochem.* **2016**, *165*, 181−191.
(21) Ribeiro, G.; Benadiba, M.; de Oliveira Silva, D.; Colquhoun, A. The novel ruthenium-γ-linolenic complex $[Ru_2(aGLA)_4Cl]$ inhibits C6 rat glioma cell proliferation and induces changes in mitochondrial membrane potential, increased reactive oxygen species generation and apoptosis in vitro. *Cell Biochem. Funct.* **2010**, *28*, 15−23.
(22) Miyake, J. A.; Benadiba, M.; Ribeiro, G.; de Oliveira Silva, D.; Colquhoun, A. Novel ruthenium-gamma-linolenic acid complex inhibits C6 rat glioma cell proliferation in vitro and in the orthotopic C6 model in vivo after osmotic pump infusion. *Anticancer Res.* **2014**, *34*, 1901−1911.
(23) Barresi, E.; Tolbatov, I.; Marzo, T.; Zappelli, E.; Marrone, A.; Re, N.; Pratesi, A.; Martini, C.; Taliani, S.; Da Settimo, F.; La Mendola, D. Two mixed valence diruthenium(II, III) isomeric complexes show different anticancer properties. *Dalton Trans.* **2021**, *50*, 9643−9647.
(24) Andrade, A.; Namora, S. F.; Woisky, R. G.; Wiezel, G.; Najjar, R.; Sertie, J. A. A.; de Oliveira Silva, D. Synthesis and characterization of a diruthenium-ibuprofenato complex comparing its anti-inflammatory activity with that of a copper(II)-ibuprofenato complex. *J. Inorg. Biochem.* **2000**, *81*, 23−27.
(25) Messori, L.; Marzo, T.; Fernandes Sanches, R. N.; Rehman, H.-U.; de Oliveira Silva, D.; Merlino, A. Unusual structural features in the lysozyme derivative of the tetrakis(acetato)chloridodiruthenium(II, III) complex. *Angew. Chem., Int. Ed.* **2014**, *53*, 6172−6175.
(26) Tolbatov, I.; Marrone, A. Kinetics of reactions of dirhodium and diruthenium paddlewheel tetraacetate complexes with nucleophilic protein sites: Computational insights. *Inorg. Chem.* **2022**, *61*, 16421−16429.
(27) Tolbatov, I.; Marrone, A. Reaction of dirhodium and diruthenium paddlewheel tetraacetate complexes with nucleophilic protein sites: A computational study. *Inorg. Chim. Acta* **2022**, *530*, 120684.
(28) Villalobos, L.; Cao, Z.; Fanwick, P. E.; Ren, T. Diruthenium(II, III) tetramidates as a new class of oxygenation catalysts. *Dalton Trans.* **2012**, *41*, 644−650.
(29) Corcos, R.; Pap, J. S.; Yang, T.; Berry, J. F. A Synthetic Oxygen Atom Transfer Photocycle from a Diruthenium Oxyanion Complex. *J. Am. Chem. Soc.* **2016**, *138*, 10032−10040.
(30) Cortijo, M.; González-Prieto, R.; Herrero, S.; Priego, J. L.; Jiménez-Aparicio, R. The Use of Amidinate Ligands in Paddlewheel Diruthenium Chemistry. *Coord. Chem. Rev.* **2019**, *400*, 213040.
(31) Osterloh, W. R.; Galindo, G.; Yates, M. J.; Van Caemelbecke, E.; Kadish, K. M. Synthesis, Structural and Physicochemical Properties of Water-Soluble Mixed-Ligand Diruthenium Complexes Containing Anilinopyridinate Bridging Ligands. *Inorg. Chem.* **2020**, *59*, 584−594.
(32) Delgado-Martínez, P.; Moreno-Martínez, L.; González- Prieto, R.; Herrero, S.; Priego, J. L.; Jiménez-Aparicio, R. Activation Method and Solvent Effects on the Structure of Paddlewheel Diruthenium Complexes. *Appl. Sci.* **2022**, *12*, 1000.
(33) Cotton, F. A.; Yokochi, A. Synthesis and Characterization of the Series of Compounds $Ru_2(O_2CMe)_x(admp)_{4-x}Cl$ (Hadmp = 2-Amino-4,6-dimethylpyridine, x = 3, 2, 1, 0). *Inorg. Chem.* **1998**, *37*, 2723−2728.
(34) Inchausti, A.; Terán, A.; Manchado-Parra, A.; de Marcos-Galán, A.; Perles, J.; Cortijo, M.; González-Prieto, R.; Herrero, S.; Jiménez-Aparicio, R. New insights into progressive ligand replacement from $[Ru_2Cl(O_2CCH_3)_4]$: synthetic strategies and variation in redox potentials and paramagnetic shifts. *Dalton Trans.* **2022**, *51*, 9708−9719.
(35) Terán, A.; Cortijo, M.; Gutiérrez, Á.; Sánchez-Peláez, A. E.; Herrero, S.; Jiménez-Aparicio, R. Ultrasound-assisted synthesis of water-soluble monosubstituted diruthenium compounds. *Ultrason. Sonochem.* **2021**, *80*, 105828.
(36) Loreto, D.; Ferraro, G.; Merlino, A. Unusual Structural Features in the Adduct of Dirhodium Tetraacetate with Lysozyme. *Int. J. Mol. Sci.* **2021**, *22*, 1496.
(37) Ferraro, G.; Pratesi, A.; Messori, L.; Merlino, A. Protein interactions of dirhodium tetraacetate: a structural study. *Dalton Trans.* **2020**, *49*, 2412−2416.
(38) Loreto, D.; Esposito, A.; Demitri, N.; Guaragna, A.; Merlino, A. Digging into protein metalation differences triggered by fluorine containing-dirhodium tetracarboxylate analogues. *Dalton Trans.* **2022**, *51*, 7294−7304.
(39) Loreto, D.; Esposito, A.; Demitri, N.; Guaragna, A.; Merlino, A. Reactivity of a fluorine-containing dirhodium tetracarboxylate compound with proteins. *Dalton Trans.* **2022**, *51*, 3695−3705.
(40) Loreto, D.; Merlino, A. The interaction of rhodium compounds with proteins: A structural Coverview. *Coord. Chem. Rev.* **2021**, *442*, 213999.
(41) Osterloh, W. R.; Galindo, G.; Yates, M. J.; Van Caemelbecke, E.; Kadish, K. M. Synthesis, Structural and Physicochemical Properties of Water-Soluble Mixed-Ligand Diruthenium Complexes Containing Anilinopyridinate Bridging Ligands. *Inorg. Chem.* **2020**, *59*, 584−594.
(42) Miskowski, V. M.; Gray, H. B. Electronic spectra of $Ru_2(carboxylate)_4^+$ complexes. Higher energy electronic excited states. *Inorg. Chem.* **1988**, *27*, 2501−2506.
(43) Vaney, M. C.; Maignan, S.; Ries-Kautt, M.; Ducruix, A. High-resolution structure (1.33 Å) of a HEW lysozyme tetragonal crystal grown in the APCF apparatus. Data and structural comparison with a crystal grown under microgravity from SpaceHab-01 mission. *Acta Crystallogr. D: Biol. Crystallogr.* **1996**, *52*, 505−517.
(44) Loreto, D.; Fasulo, F.; Muñoz-García, A. B.; Pavone, M.; Merlino, A. Unexpected imidazole coordination to the dirhodium center in a protein environment: Insights from X-ray crystallography and quantum chemistry. *Inorg. Chem.* **2022**, *61*, 8402−8405.
(45) Barral, M. C.; Gallo, T.; Herrero, S.; Jiménez-Aparicio, R.; Torres, M. R.; Urbanos, F. A. The First Open-Paddlewheel Structures in Diruthenium Chemistry: Examples of Intermediate Magnetic Behaviour between Low and High Spin in Ru_2^{5+} Species. *Chem. Eur. J.* **2007**, *13*, 10088−10095.
(46) Lozano, G.; Jimenez-Aparicio, R.; Herrero, S.; Martinez-Salas, E. Fingerprinting the junctions of RNA structure by an open-paddlewheel diruthenium compound. *RNA* **2016**, *22*, 330−338.

https://doi.org/10.1021/acs.inorgchem.2c04103
Inorg. Chem. 2023, 62, 670−674